

TNF-R family receptors, we suggest that p75 is intolerant to changes in the relative orientations of the two sites. Attempts to manually dock p75 onto both pseudosites simultaneously resulted in numerous steric clashes and implausible NGF-p75 contact distances relative to those formed at the initial sites of engagement.

The asymmetric interaction mode of p75 and NGF can be contrasted with other asymmetric receptor and ligand complexes. The immunoglobulin IgE Fc receptor complex with Fc (19), the NKG2D complex with MIC-A (20), and the complex of CNP with the natriuretic peptide receptor (21) are all asymmetric complexes containing a symmetric homodimer. However, in these cases, the ligand or receptor binds directly on the two-fold symmetry axis; thereby, it sterically imposes the asymmetry through blockade of the binding site. The p75-NGF complex is distinct in that the receptor binds away from the symmetry axis of NGF, which leaves the mirror-image binding site completely accessible for another receptor interaction. Therefore, an allosteric mechanism is required in order to disable the pseudosites. A possible functional rationale for this mechanism is to preserve an open face of NGF that could engage a second, but different, receptor and form a heterotrimeric complex.

The asymmetric NGF-p75 complex structure now helps provide a framework for interpreting the voluminous body of functional data published on NT signaling through p75 and Trk (1–3, 5, 7–9). On the basis of our structural and biochemical data, we propose that one mechanism of p75 activation is through NT-induced dissociation of a receptor dimer. This mechanism is consistent with some experimental data (1, 5, 8), such as a cross-linking study showing that apoptotic induction by p75 requires monomerization, whereas enforced dimerization is inhibitory (22). The NT-induced p75 disassociation mechanism does not exclude the possibility that other receptor configurations or oligomers may initiate signaling, dependent on the cellular environment. For instance, p75 alone, p75 as dependence receptor, p75 with Trks, and p75 with Nogo receptor may each have signaling mechanisms distinct from the NT-p75 complex. This could explain the complexity of p75 signaling. For example, in the same type of neuronal cells, NGF binding to p75 inactivates Rho (23), whereas binding of Nogo to the NgR-p75 complex results in Rho activation (24).

The asymmetric NGF-p75 complex lends some mechanistic insight into the role of p75 in coordinating with Trk. The TrkA-NGF complex is known to comprise two NGF monomers and two TrkA molecules in a symmetric 2:2 stoichiometry (11). Although Trk and p75 are mutually exclusive on the same side of NGF because of the clash between the Trk D5 domain and the p75 CRD2-CRD3 junction, NGF is structurally capable of binding TrkA and p75 simultaneously on opposite sides to form a trimolecular complex (Fig. 4D). Of note, the TrkA binding site on

NGF, composed of the central β sheet, is unaffected by the conformational changes induced by p75; these changes are localized to the distal loops of NGF (Fig. 4A). The structural possibility of the trimolecular complex supports an equilibrium between p75 dimers, p75-NT complexes, NT-Trk complexes, and trimolecular Trk-NT-p75 signaling complexes (Fig. 4D) that would be dictated by the relative expression levels of each component and by the concentration of NT (7, 8). Further, the p75-induced neurotrophin conformational changes on the side of the pseudosites could be a mechanistic glimpse of the long-suspected allostery by which p75 modulates Trk ligand affinity and specificity for neurotrophins.

References and Notes

1. M. Bothwell, *Annu. Rev. Neurosci.* **18**, 223 (1995).
2. M. Bibbel, Y. A. Barde, *Genes Dev.* **14**, 2919 (2000).
3. G. R. Lewin, Y. A. Barde, *Annu. Rev. Neurosci.* **19**, 289 (1996).
4. C. F. Ibanez, *Trends Biotechnol.* **13**, 217 (1995).
5. M. V. Chao, *Nature Rev. Neurosci.* **4**, 299 (2003).
6. G. Dechant, Y. A. Barde, *Nature Neurosci.* **5**, 1131 (2002).
7. B. L. Hempstead, *Curr. Opin. Neurobiol.* **12**, 260 (2002).
8. E. J. Huang, L. F. Reichardt, *Annu. Rev. Biochem.* **72**, 609 (2003).
9. S. Rabizadeh, D. E. Bredesen, *Cytokine Growth Factor Rev.* **14**, 225 (2003).
10. B. L. Hempstead, D. Martin-Zanca, D. R. Kaplan, L. F. Parada, M. V. Chao, *Nature* **350**, 678 (1991).
11. C. Wiesmann, M. H. Ultsch, S. H. Bass, A. M. de Vos, *Nature* **401**, 184 (1999).

12. Materials and methods are provided in Supporting Online Material (SOM).
13. P. M. Grob, A. H. Ross, H. Koprowski, M. Bothwell, *J. Biol. Chem.* **260**, 8044 (1985).
14. S. Jing, P. Tapley, M. Barbacid, *Neuron* **9**, 1067 (1992).
15. N. Q. McDonald *et al.*, *Nature* **354**, 411 (1991).
16. D. W. Banner *et al.*, *Cell* **73**, 431 (1993).
17. M. J. Boulanger, A. J. Bankovich, T. Kortemme, D. Baker, K. C. Garcia, *Mol. Cell* **12**, 577 (2003).
18. A. Rodriguez-Tebar, G. Dechant, Y. A. Barde, *Neuron* **4**, 487 (1990).
19. S. C. Garman, B. A. Wurzburg, S. S. Tarchevskaya, J. P. Kinet, T. S. Jardetzky, *Nature* **406**, 259 (2000).
20. P. Li *et al.*, *Nature Immunol.* **2**, 443 (2001).
21. X. He, D. Chow, M. M. Martick, K. C. Garcia, *Science* **293**, 1657 (2001).
22. J. J. Wang *et al.*, *J. Neurosci. Res.* **60**, 587 (2000).
23. T. Yamashita, K. L. Tucker, Y. A. Barde, *Neuron* **24**, 585 (1999).
24. K. C. Wang, J. A. Kim, R. Sivasankaran, R. Segal, Z. He, *Nature* **420**, 74 (2002).
25. We thank A. M. de Vos (Genentech, Inc.) for the gift of recombinant human NGF, NT-4/5 and NT-3; M. Boulanger for assistance with MALS; W. Mobley for helpful discussions and mouse NGF; and B. Hempstead and C. F. Ibanez for critically reading the manuscript. K.C.G. is supported by the American Heart Association, Christopher Reeve Paralysis Foundation, Keck Foundation, and NIH. X.H. is supported by the Fritz Krauth Memorial Fellowship from Paralyzed Veterans of America, Spinal Cord Research Foundation. The coordinates and structural factors have been deposited in the Protein Data Bank with accession number 1SG1.

Supporting Online Material

www.sciencemag.org/cgi/content/full/304/5672/870/DC1

Materials and Methods

Table S1

20 December 2003; accepted 4 March 2004

Periodic Signaling Controlled by an Oscillatory Circuit That Includes Protein Kinases ERK2 and PKA

Mineko Maeda,¹ Sijie Lu,^{2*} Gad Shaulsky,³ Yuji Miyazaki,¹ Hidekazu Kuwayama,⁴ Yoshimasa Tanaka,⁴ Adam Kuspa,^{2,3} William F. Loomis^{5†}

Self-regulating systems often use robust oscillatory circuits. One such system controls the chemotactic signaling mechanism of *Dictyostelium*, where pulses of adenosine 3',5'-monophosphate (cAMP) are generated with a periodicity of 7 minutes. We have observed spontaneous oscillations in activation of the mitogen-activated protein (MAP) kinase ERK2 that occur in phase with peaks of cAMP, and we show that ERK2 modulates cAMP levels through the phosphodiesterase RegA. Computer modeling and simulations of the underlying circuit faithfully account for the ability of the cells to spontaneously generate periodic pulses during specific stages of development. Similar oscillatory processes may occur in cells of many different species.

During development, a few *Dictyostelium* cells spontaneously emit pulses of cAMP, and surrounding cells respond within a minute by releasing more of the signal. When observed in monolayers, cAMP relay leads to nondissipating target and spiral patterns that expand through the field with a period of 6 to 7 min, much like self-propagating waves in excitable fields (1, 2). The period decreases

from about 8 min to 6 min as the cells develop (3). The phase can be set by exogenous cAMP, but the period depends on endogenous molecular interactions within individual cells. Rapid activation and delayed inhibition of adenylyl cyclase could account for periodic production of cAMP, and there is considerable evidence that such processes occur in *Dictyostelium*. After a pulse of exoge-

nous cAMP, the MAP kinase ERK2 and the cAMP-dependent protein kinase A (PKA) are

¹Department of Biology, Graduate School of Science, Osaka University, Machikaneyama-cho 1-16, Toyonaka, Osaka 560-0043, Japan. ²Department of Biochemistry and Molecular Biology, ³Department of Molecular and Human Genetics, Baylor College of Medicine, Houston TX 77030, USA. ⁴Institute of Biological Sciences, University of Tsukuba, Tsukuba, Ibaraki 305-8572, Japan. ⁵Division of Biological Sciences, University of California, San Diego, La Jolla, CA 92093, USA.

both activated for several minutes but then return to basal levels (4, 5). Cells lacking PKA return more slowly to basal ERK2 activity, whereas constitutive PKA activity leads to greatly reduced ERK2 activity after stimulation with cAMP (6, 7). These results

*Present address: Department of Blood and Marrow Transplantation, M. D. Anderson Cancer Center, Houston, TX 77030, USA.

†To whom correspondence should be addressed. E-mail: wloomis@ucsd.edu

Fig. 1. (A and B) Response to cAMP stimulation. Cells of various strains were developed for 8 hours in suspension, with pulses of 100 nM cAMP given every 6 min for the last 4 hours (25). Cells were then washed and stimulated with 1 μM 2'-deoxy-cAMP. cAMP accumulation was measured in samples taken at 1-min intervals. Genotypes of the various strains are indicated. Results are representative of three or more independent experiments with each strain.

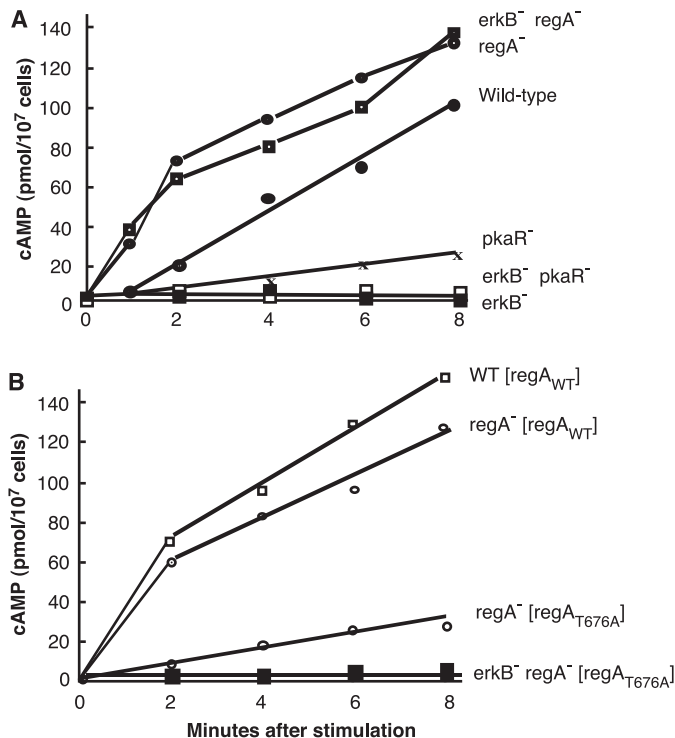
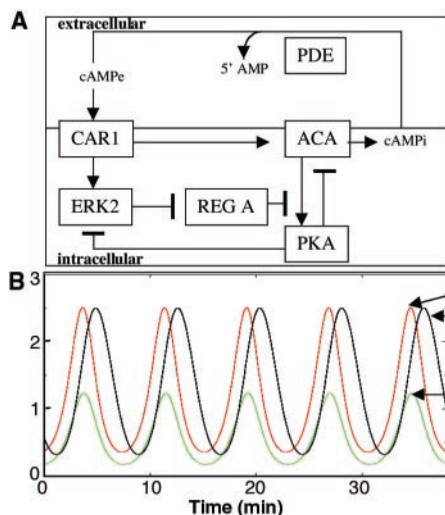


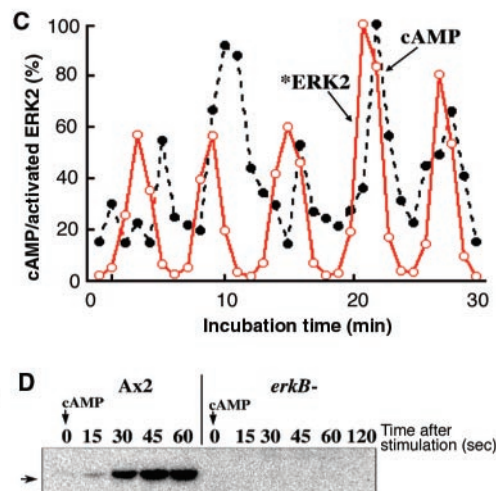
Fig. 2. Spontaneous oscillations. (A) The circuit that generates oscillations is modified from Laub and Loomis (13). Arrows indicate activation; bars indicate inhibition. PDE is the secreted phosphodiesterase that hydrolyzes extracellular cAMP (cAMPe). CAR1 is the cAMP receptor; ACA is the aggregation adenylyl cyclase; PKA is the cAMP-dependent protein kinase; ERK2 is the MAP kinase; and RegA is the phosphodiesterase that hydrolyzes internal cAMP (cAMPi). Connecting intermediates, such as trimeric G protein, phosphatidylinositol 3-kinase, CRAC, and Pianissimo, are not included in the present analyses, and the proposed interactions need not be direct. (B) Output of the circuit simulation of cells at 4 hours of development. Periodic changes in ERK2 activity and the internal and external levels of cAMP are indicated (arbitrary units). (C) Measured changes in phospho-ERK2 and cAMP in pulse-developed cells that were washed and resuspended at 5 × 10⁷ cells/ml. Samples were taken at 1-min intervals. The NIH Image package was used to quantify the level of phospho-ERK. Results are representative of three inde-



indicate that the activities of these protein kinases are connected in a molecular circuit.

Many aspects of the signal transduction pathway from the seven-transmembrane G protein-coupled cAMP receptor, CAR1, to the activation of the membrane-bound adenylyl cyclase, ACA, have been established in *Dictyostelium* both biochemically and genetically (8, 9). Most of the newly synthesized cAMP is released to relay the signal, but PKA is also activated by intracellular cAMP. In each oscillation, cAMP levels increase for about 3 min and then return to basal levels as the result of transient activation of ACA and the action of the extracellular and intracellular cAMP phosphodiesterases PDE and RegA (1, 2, 10, 11). The signal transduction pathway(s) that result in attenuation of the response are not yet fully understood, but it is known that ligand-bound CAR1 not only activates ACA but also leads to transient activation of ERK2, which has been shown to be essential for the accumulation of cAMP (4, 12). It was suggested that ERK2 might be necessary for the inhibition of the internal phosphodiesterase RegA, which otherwise would hydrolyze newly made cAMP, leading to a futile cycle and failure to activate PKA (13).

In a screen for suppressors of the aggregateless phenotype of *erkB*⁻ cells, we found one strain in which the *regA* gene was disrupted. Unlike the parent strain, the double mutant (*erkB*⁻ *regA*⁻) is able to aggregate and form spores, but only if the amoebae are incubated as a dense lawn where aggregation can occur as the result of adhesion of randomly moving cells. At lower cell densities, aggregation does not occur and the cells show no evidence for relay of the chemotactic sig-



pendent experiments. (D) Samples from pulse-developed wild-type (Ax2) and *erkB*⁻ null cells were collected after treatment with 100 nM cAMP and analyzed on Western blots with antibodies to phospho-p44/p42 MAP kinase to establish the specificity of the antibodies to ERK2 in *Dictyostelium*.

nal. The *erkB*⁻ phenotype was also suppressed by targeted disruption of *regA*, confirming the genetic relationship. Inactivation of *regA* restored the ability of *erkB*⁻ cells to accumulate cAMP after stimulation (Fig. 1A). Relative to wild-type cells, both the *erkB*⁻ *regA*⁻ double mutant and the *regA*⁻ null strain accumulated more cAMP during the first few minutes after stimulation, probably as a result of the reduced levels of internal phosphodiesterase. Although double mutants lacking ERK2 (*erkB*⁻) with constitutive PKA because of targeted disruption of the gene encoding the regulatory subunit of PKA (*pkaR*⁻) were found to aggregate and develop to the finger stage, they did not accumulate cAMP after stimulation (Fig. 1A). Wild-type cells in which *pkaR* was disrupted also accumulated very little cAMP after stimulation (Fig. 1A). A strain carrying a null mutation in *pkaR* was previously shown to accumulate almost no cAMP throughout early development (14). These results show that ERK2 is not essential for activation of ACA and that RegA limits the accumulation of cAMP. Moreover, it appears that constitutive PKA activity precludes accumulation of cAMP either directly or indirectly and is sufficient to allow development up to the finger stage in

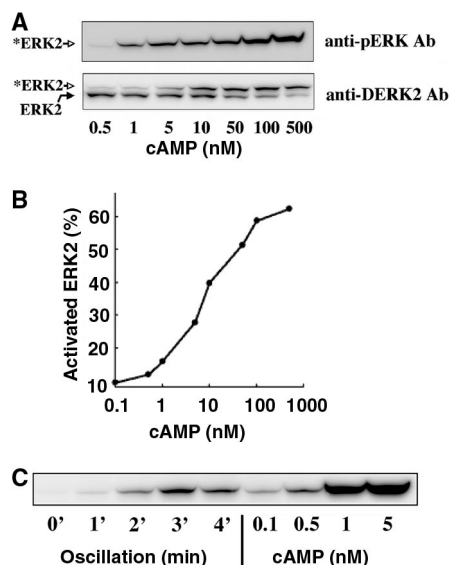


Fig. 3. ERK2 activation in response to cAMP. (A) Pulse-developed wild-type cells were treated with various concentrations of cAMP and samples collected after 30 s for analyses on Western blots using antibodies to either phospho-p44/p42 MAP kinase (specific to phosphorylated ERK2 in *Dictyostelium*) or *Dictyostelium* ERK2 (anti-DERK2), which recognizes both unphosphorylated and phosphorylated ERK2 (*ERK2). (B) The proportion of activated ERK2 measured with anti-DERK2 was calculated as percentage of total ERK2 after stimulation with various levels of cAMP. (C) Levels of phospho-ERK2 during a spontaneous oscillation were compared to levels of phospho-ERK2 30 s after treatment with 0.1 to 5 nM cAMP.

the absence of cAMP accumulation, as previously reported (15–17).

ERK2 may directly inhibit phosphodiesterase activity by phosphorylation of RegA. There are several potential MAP kinase target sites near the catalytic domain at the C-terminal sequence of RegA. We used site-directed mutagenesis to convert Thr⁶⁷⁶ to Ala (T676A) to preclude phosphorylation and expressed the mutant protein in *regA*⁻ null cells. We also transformed wild-type *regA* into either a wild-type background or a *regA*⁻ null background. Cells expressing wild-type *regA* accumulated cAMP to the same levels seen in wild-type cells (Fig. 1). However, *regA*⁻ cells expressing the T676A variant of RegA accumulated less than 15% as much cAMP, consistent with reduced inhibition of the phosphodiesterase activity (Fig. 1B). Cells of the double mutant *erkB*⁻ *regA*⁻ transformed with the T676A construct also failed to accumulate cAMP after stimulation (Fig. 1B).

A circuit including CAR1, adenylyl cyclase, cAMP phosphodiesterases, and the two protein kinases has been proposed on the basis of biochemical and genetic evidence (13, 18). Because it is now clear that ERK2 does not play a direct role in activation of adenylyl cyclase, we have appropriately modified the circuit. Moreover, we modified the model such that PKA activity is responsible for the inhibition of activation of adenylyl cyclase based on the prolonged activity of ACA after cAMP stimulation *pkaC*-null cells (19). We analyzed the circuit shown in Fig. 2A with the use of differential equations representing activation and inactivation kinetics for each component (table S1). Numerical solution of the equations predicts that ERK2 activity oscillates with a 7-min period, in phase with changes in cAMP (Fig. 2B). To test these predictions, we used antibodies that specifically recognize *Dictyostelium* phospho-ERK2 (anti-phospho-ERK) and found that activated ERK2 spontaneously oscillated with a period of about 6 min (Fig. 2C). cAMP levels also showed spontaneous oscillations reaching peaks slightly after the peaks in activated ERK2 (Fig. 2C, dashed line). The specificity of the antibody was demonstrated by analyzing the kinetics of appearance of phospho-ERK2 after stimulation of wild-type and *erkB*⁻

null cells with exogenous cAMP (Fig. 2D).

To assess the level of activated ERK2 during spontaneous oscillations, we pulsed developed cells with different levels of cAMP and analyzed samples 30 s after stimulation. We used both anti-phospho-ERK and antibodies raised against a 27-amino acid peptide from the C terminus of ERK2, which recognize both the slower migrating phospho-ERK2 and unphosphorylated ERK2 (Fig. 3A). Both methods for estimating the amount of activated ERK2 showed that phospho-ERK2 increases between 1 and 100 nM (Fig. 3B). By comparing the levels of activated ERK2 seen during spontaneous oscillations to those in cells treated with exogenous cAMP, we found that peak activity corresponded to that induced by 1 nM cAMP (Fig. 3C).

Previously, we showed that cAMP failed to activate ERK2 in a *carA*⁻ strain lacking the receptor CAR1 but activated ERK2 normally in an *acaA*⁻ strain lacking the major adenylyl cyclase (4, 7). Activation in a *gfpA*⁻ strain lacking Gβ was attenuated but still clearly observable (4, 6). These observations were all confirmed using anti-phospho-ERK. Strains carrying null mutations in *carA*, *gfpA*, or *acaA* failed to show spontaneous oscillations in ERK2 activation, supporting the predictions of the circuit model (fig. S1).

Although stable oscillations in ERK2 were routinely observed in cells that had been pulsed with cAMP for 4 hours in suspension, they were never seen in growing cells or in cells that had been developed for 7 hours or more (fig. S2). At the start of development, adenylyl cyclase activity is low but accumulates over the following 8 hours (3). Spontaneous oscillations in ACA activity are first observed at 3.5 hours of development, continue for about 3 hours, and then cease. In our computer simulations, we mimicked developmental changes in ACA by ramping the maximal activity up by a factor of 6 during the first 4 hours. Oscillations in both ACA and ERK2 were not seen until after 3 hours, increased in amplitude until 4.5 hours, and then remained constant. Attenuation of the spontaneous oscillations could be mimicked by reducing the level of RegA by a factor of 5 over the first 7 hours (Fig. 4). It is known that RegA is subject

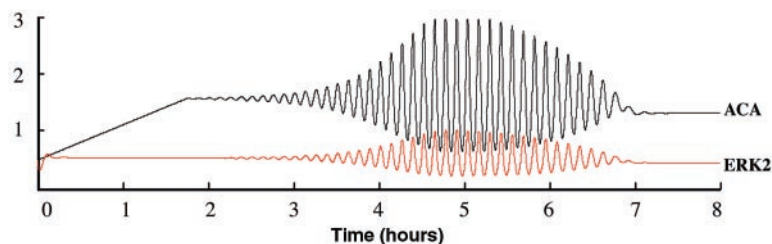


Fig. 4. Spontaneous oscillations during development. Output of the circuit simulation of cells in which the maximum activity of ACA increases by a factor of 6 during the first 4 hours of development and the maximum activity of the internal phosphodiesterase RegA decreases by a factor of 5 over the first 7 hours. Strong oscillations in ACA (arbitrary units) only occurred between 4 and 6 hours of development. Oscillations of activated ERK2 and other components of the circuit were also restricted to this developmental stage.

to regulated degradation between 4 and 12 hours of development (20). The strong oscillation seen only between 4 and 6 hours of development during the simulation is strikingly similar to the observations of Gerisch *et al.* (3).

The oscillatory circuit that we have modeled is based on only six components and yet adequately accounts for the observed spontaneous oscillation of ERK2 that occurs in phase with periodic signaling by cAMP (Fig. 2). Complete loss through genetic disruption of any one of the components results in a lack of periodic behavior. The model predicts that partial loss of some of the enzymes will affect the amplitude of the oscillations without substantially affecting the period. This prediction could be tested with carefully chosen site-directed mutations. Although the present model does not attempt to account for other aspects of signal relay, such as adaptation, it shows how cells become robustly entrained to a 6- to 7-min cycle as soon as the components are put in place. An alternative model that also involves a positive feedback loop in which secreted cAMP binds the CAR1 receptor, leading to activation of adenylyl cyclase, invokes receptor desensitization to produce sustained oscillations (21, 22). It is possible that both mechanisms play a role in signal relay.

The protein kinases ERK and PKA also regulate cAMP phosphodiesterase activity in mammalian cells. ERK phosphorylates the catalytic domains of PDE4 families B, C, and D, leading to inhibition of the long isoforms (23). When cAMP accumulates and activates PKA, ERK-dependent inhibition is overcome (24). This circuit could lead to oscillations similar to those seen in *Dictyostelium*. Because these components have been conserved throughout evolution of the animal kingdom, it seems reasonable that other species have such an oscillator in place and continue to use it for diverse functions.

References and Notes

1. G. Gerisch, U. Wick, *Biochem. Biophys. Res. Commun.* **65**, 364 (1975).
2. K. Tomchik, P. N. Devreotes, *Science* **212**, 443 (1981).
3. G. Gerisch, D. Malchow, W. Roos, U. Wick, *J. Exp. Biol.* **81**, 33 (1979).
4. M. Maeda *et al.*, *J. Biol. Chem.* **271**, 3351 (1996).
5. M. M. Behrens, M. Juliani, J. Maia, *Biochem. Int.* **13**, 221 (1986).
6. M. Knetsch *et al.*, *EMBO J.* **15**, 3361 (1996).
7. L. Aubry, M. Maeda, R. Insall, P. N. Devreotes, R. A. Firtel, *J. Biol. Chem.* **272**, 3883 (1997).
8. C. A. Parent, P. N. Devreotes, *Annu. Rev. Biochem.* **65**, 411 (1996).
9. L. Aubry, R. Firtel, *Annu. Rev. Cell Dev. Biol.* **15**, 469 (1999).
10. W. Roos, C. Scheidegger, G. Gerisch, *Nature* **266**, 259 (1977).
11. G. Shaulesky, D. Fuller, W. F. Loomis, *Development* **125**, 691 (1998).
12. J. E. Segall *et al.*, *J. Cell Biol.* **128**, 405 (1995).
13. M. Laub, W. F. Loomis, *Mol. Biol. Cell* **9**, 3521 (1998).
14. K. Abe, K. Yanagisawa, *Dev. Biol.* **95**, 200 (1983).
15. B. Wang, A. Kuspa, *Science* **277**, 251 (1997).
16. C. Anjard, F. Soderbom, W. F. Loomis, *Development* **128**, 3649 (2001).
17. N. Iranfar, D. Fuller, W. F. Loomis, *Eukaryot. Cell* **2**, 664 (2003).
18. D. Wessels *et al.*, *Mol. Biol. Cell* **11**, 2803 (2000).

19. S. Mann *et al.*, *Dev. Biol.* **183**, 208 (1997).
20. S. Mohanty *et al.*, *Genes Dev.* **15**, 1435 (2001).
21. J.-L. Martiel, A. Goldbeter, *Biophys. J.* **52**, 807 (1987).
22. A. Goldbeter, *Nature* **420**, 238 (2002).
23. G. Baillie, S. MacKenzie, I. McPhee, M. Houslay, *Br. J. Pharmacol.* **131**, 811 (2000).
24. G. Baillie, S. MacKenzie, M. Houslay, *Mol. Pharmacol.* **60**, 1100 (2001).
25. See supporting data on Science Online.
26. We thank S. Payne and W.-J. Rappel for assistance with the circuit simulations and M. Behrens for discussions. D. Ikeno made contributions to these studies. Supported by NIH grants GM62350

(W.F.L.) and GM52359 (A.K.), an NSF Biocomplexity Grant, and Ministry of Education, Science and Culture of Japan grants 12640633 and 13024248 (M.M.).

Supporting Online Material

www.sciencemag.org/cgi/content/full/304/5672/875/DC1
 Materials and Methods
 Figs. S1 and S2
 Table S1
 References

12 December 2003; accepted 5 April 2004

Cognitive Inflexibility After Prefrontal Serotonin Depletion

H. F. Clarke,¹ J. W. Dalley,¹ H. S. Crofts,¹ T. W. Robbins,¹ A. C. Roberts^{2*}

Serotonergic dysregulation within the prefrontal cortex (PFC) is implicated in many neuropsychiatric disorders, but the precise role of serotonin within the PFC is poorly understood. Using a serial discrimination reversal paradigm, we showed that upon reversal, selective serotonin depletion of the marmoset PFC produced perseverative responding to the previously rewarded stimulus without any significant effects on either retention of a discrimination learned preoperatively or acquisition of a novel discrimination postoperatively. These results highlight the importance of prefrontal serotonin in behavioral flexibility and are highly relevant to obsessive-compulsive disorder, schizophrenia, and the cognitive sequelae of drug abuse in which perseveration is prominent.

Serotonin [5-hydroxytryptamine (5-HT)] is implicated in cognition and impulsivity and is of particular relevance to our understanding of the psychopathology and treatment of psychiatric disorders such as depression, schizophrenia, and obsessive compulsive disorder (OCD). In all of these disorders, local abnormalities in prefrontal cortex (PFC) structure (1), neurochemistry (2), or activation (3) have been identified, and as is consistent with prefrontal dysfunction, cognitive inflexibility is a prominent feature. Moreover, drugs such as ecstasy (4) and amphetamine (5) have been shown to impair cortical 5-HT neurotransmission, but the functional consequences of such serotonin dysregulation are not known.

Two approaches used to study the effect of central 5-HT on behavior and cognition are

dietary tryptophan depletion in humans (6) and destruction of the ascending serotonergic projections in animals, using the selective neurotoxin 5,7-dihydroxytryptamine (5,7-DHT) (7). However, neither approach can differentiate between the roles of 5-HT in distinct forebrain structures, although there is indirect evidence that not all forebrain structures are equally modulated by 5-HT. Tryptophan depletion in humans has little effect on the performance of tasks activating the dorsolateral region of the PFC, such as spatial working memory or planning (6). However, tryptophan depletion does impair performance on visual discrimination reversal tasks (6, 8), on which performance is disrupted by orbitofrontal cortex (OFC) lesions in nonhuman primates (9, 10) and humans (11). There are therefore similarities between tasks that depend on OFC function and tasks that are affected by tryptophan depletion, suggesting a role for 5-HT in processes mediated by the OFC.

The present study investigated the effects of selective prefrontal depletion of 5-HT in pri-

¹Department of Experimental Psychology, ²Department of Anatomy, University of Cambridge, Downing Street, Cambridge, UK.

*To whom correspondence should be addressed. E-mail: acr4@cam.ac.uk

Table 1. Mean total error scores and SEM values (square root–transformed) for control and lesion groups at each experimental stage.

	D1	D2	SUR	D2 Retention	D3	Rev 1	Rev 2	Rev 3	Rev 4
Control ± SEM	6.3 ± 1.8	10.4 ± 2	2.01 ± 2	9.1 ± 3.7	17.1 ± 2.5	12.2 ± 2.3	10.3 ± 1	7.1 ± 1.0	
Lesion ± SEM	6.6 ± 2.2	8.8 ± 1.4	3.5 ± 2.2	7.0 ± 2.4	17.8 ± 3	17.5 ± 2	17.1 ± 3	11.2 ± 2	